

Mass-Transfer Process of Galactic Compact Binaries

Zi-han Zhang^{1,*}, Bin Liu^{1,†} and Jie Yang^{1,2}

¹*School of Physical Science and Technology, Lanzhou University, Lanzhou 730000, China and*

²*Lanzhou Center for Theoretical Physics, Key Laboratory of Theoretical Physics of Gansu Province, Lanzhou University, Lanzhou 730000, China*

(Dated: April 27, 2023)

In this paper we focus on the effect of mass transfer between compact binary stars like neutron star–neutron star (NS-NS) system and neutron star–white dwarf (NS-WD) system. We adopt mass quadrupole formula with post-Newtonian approximation to calculate the gravitational wave (GW) radiation and orbit evolution. Two kinds of mass transfer process are considered here. One is the tidal disruption model where the less dense star orbits into the Roche limit and its mass flows toward to the other star as a beam of incompressible fluid, and the other is common envelope model where we divide the transferring mass into the mass-inflow of envelope and the the envelope itself winding in the Roche lobe of the binary stars. Viewing the envelope as a background, the GW by its spin can be calculated as a pulsar. Assuming a mass-inflow parameter, we eventually obtain the radiation power and corrected gravitational wave form (GWF) templates for different initial mass ratios, which are mainly captured by the inspiral duration and strain and of the GWs.

I. INTRODUCTION

Inner Milky Way compact binaries are an important sources of celestial GW detection [1, 2]. They are within the sensitive frequency band (0.1 mHz-0.1 Hz) of detectors and the are rich in number [3, 4]. GW signals from these sources contain a wealth of information about their formation and evolution, mass transfer and the equation of state [5]. Establishing an accurate gravitational wave form (GWF) template library for close compact binary stars with Roche lobe overflow, material exchange and other influence can not only help to analyse waveforms, but also benefit data processing for numerous compact binaries, so that their noise can be reduced when identifying other singles [6–9].

Different GW sources of compact binaries produce GWs with different strengthes and frequencies. Binaries sources include BH-BH, BH-NS, NS-NS, NS-WD, and WD-WD [10]. The GW signals they produce are weakened in turn, but events of merger rate increases. The existing space-based GW detectors LISA, TaiJi, TianQin, DECIGO, and ground-based detectors LIGO and Virgo, etc. are different in sensitive strength and frequency bands. Therefore, it is necessary to prepare the corresponding GW template in advance to distinguish them generated by the sources of various compact binary systems, which region is detected. Among them, the NS-NS system and the NS-WD system, at the current detection range of 10^2Mpc [11, 12], are expected to observe several or even more than a dozen cases of double neutron star merger GW signals every year in the future.

The post-Newtonian approximation [13–17] is widely used in the approximate solutions of the Einstein field

equation, expanding it to higher order terms than Newtonian to make the solution more precise. It plays a significant role in theoretical calculation of GWs from slow-moving objects in weak fields, which are the most cases in binary systems.

The theoretical framework of post-Newtonian approximation approach to a binary system consists of two parts: binary dynamics and GW emissions [18]. The post-Newtonian dynamical equations of this two-body problem generally take two forms [19]: the Hamiltonian form and the Lagrangian form. In some situations the former may give chaotic orbits, while the latter is always compatible with Keplerian-type parametric solutions that we are used to. These are also crucial parameters in calculating the GWF of binaries inspiraling along PN accurate eccentric orbits [20]. So our procedure is to first solve the dynamics equations, and then plug the orbit into GW formula to obtain the waveform.

GW signals generated by the inspiral and merger of binary stars are the main targets of future celestial GW detectors. This paper discusses the evolution of NS-NS and NS-WD binary systems in the context of general relativity, and calculates the their GWFs using the post-Newtonian approximation. Notice that the the mass range of NSs is generally between $1.35 \sim 2.1 M_\odot$, and the radius is between $1.4 \times 10^{-5} \sim 3.3 \times 10^{-5} R_\odot$, while WDs are much more loose with mass range generally between $0.2 \sim 1.4 M_\odot$, and radius between $8 \times 10^{-3} \sim 2 \times 10^{-2} R_\odot$, so more attention is paid on the NS-WD binaries when we investigate the effect of mass transfer [21–23].

As for the outcome of NS-NS merger, it varies depending on the total mass, total angular momentum, mass ratio, equation of state and other conditions. Usually the total mass of a inner Milky Way NS-NS binary is within $2.5 \sim 2.88 M_\odot$, and the mass ratio between 1.1 to 1.3. When the total mass reaches to $3.15 \sim 4.10 M_\odot$, the binary may immediately collapse into a black hole with angular momentum density $a = J/M$ around $0.7 \sim 0.8$

* zhangzihan19@lzu.edu.cn

† liubin2020@lzu.edu.cn

[24, 25]. The material of its accretion disk will eventually fall into the black hole along with the GW radiation and angular momentum loss in the ringdown phase. That is the situation we take into consideration at the end of evolution, whose GW can be calculated by black hole perturbation theory.

The theoretical analysis and numerical computation in this paper are arranged in these following sections. In Sec.II, we briefly review the standard routine to simplify the independent variables in Einstein field equation in the TT gauge where the final metric perturbation $h_{\mu\nu}$ has only two independent variables $h_+(t)$ and $h_\times(t)$. In Sec.III, we give the evolution equation of the binary system, and use post-Newtonian approximation of Hamiltonian form to calculate the trajectory and radiation power. In Sec.IV, we propose the tidal disruption model[26–28], and common envelope model[29, 30], where the GW of the mass-background is treated as a pulsar[31, 32]. Finally, waveforms with respect to different mass-inflow parameters and initial mass ratios are discussed. All calculations are in natural units where $G = c = 1$.

II. TWO POLARIZATION MODES

We begin with the Einstein field equation (EFE), where the metric $g_{\mu\nu}$ is a symmetric (0,2) tensor with generally 10 independent variables constrained by 10 correlated second-order nonlinear partial differential equations

$$G_{\mu\nu}(g_{\mu\nu}) = \kappa T_{\mu\nu}. \quad (1)$$

Due to the conservation of energy-momentum tensor, 4 constrains are eliminated by Bianchi identity

$$\nabla^\mu G_{\mu\nu} = 0. \quad (2)$$

The independence of coordinates also loses 4 constrains, leaving only two constrains with actual physical meaning. To obtain the specific metric with those two variables, supplemental constrains are required along with Einstein field equation, which are the harmonic gauge and Transverse-Traceless (TT) gauge [33] as

$$h_{ij}^{TT} = h_{ij}^{TT}, \quad \sum_i h_{ii}^{TT} = 0, \quad \sum_i \nabla_i h_{ij}^{TT} = 0. \quad (3)$$

Writing down the spacetime metric as $g_{\mu\nu} = \eta_{\mu\nu} + h_{\mu\nu}$, where $\eta_{\mu\nu}$ is the flat metric and $h_{\mu\nu}$ are small perturbations, the former reduces EFE to

$$\square \tilde{h}_{\mu\nu} = -2\kappa T_{\mu\nu}, \quad (4)$$

$$\tilde{h}_{\mu\nu} = h_{\mu\nu} - \frac{h}{2}\eta_{\mu\nu}. \quad (5)$$

Choosing the GW transverses to z axis, the latter gives

$$h_{ab}^{TT}(t, z) = \begin{pmatrix} C_+ & C_\times \\ C_\times & -C_+ \end{pmatrix} \cos[\omega(t - \frac{z}{c})], \quad (6)$$

where $a, b = 1, 2$, z is the direction of propagation, and C is the time independent strength of GW, then we can get the metric

$$h_{ab} \equiv C_{ab} \cdot \cos[\omega(t - \frac{z}{c})], \quad (7)$$

$$ds^2 = -c^2 dt^2 + dz^2 + (1 + h_+)dx^2 + (1 - h_+)dy^2 + 2h_\times dx dy, \quad (8)$$

based on this metric, we can get the equation of $h_+(t)$ and $h_\times(t)$ by calculating the perturbation of metric tensor.

III. BINARIES' EVOLUTION AND GWF

A. Mass Quadrupole Tensor

We use $[M]$ to measure time, length, and mass in natural units. The masses of the two stars are m_1 and m_2 respectively where $m_1 \geq m_2$. Setting the rotation plane to be xOy plane, we calculate the mass quadrupole tensor and its third order derivative.

$$\ddot{Q}_{xx} = \beta b(2 \sin 2\theta + 3e \sin \theta \cos^2 \theta), \quad (9)$$

$$\ddot{Q}_{yy} = -\beta b[2 \sin 2\theta + e \sin \theta(1 + 3 \cos^2 \theta)], \quad (10)$$

$$\ddot{Q}_{xy} = \ddot{Q}_{yx} = -\beta b[2 \cos 2\theta - e \cos \theta(1 - 3 \cos^2 \theta)], \quad (11)$$

where e is the eccentricity, θ is the anomaly, a is the winding semi-major axis, and $b \equiv (1 + e \cos \theta)^2$. And we have

$$\dot{\theta} = \frac{[(m_1 + m_2)a(1 - e^2)]^{\frac{1}{2}}}{r^2}, \quad (12)$$

$$\beta^2 \equiv \frac{4m_1^2 m_2^2 (m_1 + m_2)}{a^5 (1 - e^2)^5}. \quad (13)$$

The radiation power P only depends on \ddot{Q} :

$$P = -\frac{dE}{dt} = \frac{1}{5}(\ddot{Q}_{ij}\ddot{Q}^{ij} - \frac{1}{3}\ddot{Q}_i^i \ddot{Q}_j^j). \quad (14)$$

According to the expression of the mass quadrupole tensor, we can get the average radiation power in a period

$$\bar{P} = \frac{32}{5} \frac{m_1^2 m_2^2 (m_1 + m_2)}{a^5 (1 - e^2)^{\frac{7}{2}}} (1 + \frac{73}{24}e^2 + \frac{37}{96}e^4). \quad (15)$$

B. Post-Newtonian Approximation

Usually the pressure and temperature are negligible for regular compact binaries in weak fields [13, 34]. Here we only consider the dynamic equations of compact binaries due to mass distribution. Parameters are introduced as: the total mass of system $M = m_1 + m_2$, the lost mass $\delta m = m_2^{(0)} - m_2$ of m_2 , where $m_2^{(0)}$ is the initial mass of star 2 and m_2 is the final mass. $\mu = m_1 m_2 / M$, $\nu = (m_1 - m_2) / M$, and $\eta = (1 - \nu^2) / 4$, $q = m_1 / m_2$. Let \mathbf{x} and

\mathbf{v} be the relative coordinate vector and velocity vector, defining the unit vector $\mathbf{n} = \mathbf{x}/r$ where r is the distance between two stars.

These post-Newtonian dynamics equations for the two-body problem have can be written as Hamiltonian form or Lagrangian form [19]. In harmonic gauge, the expansion of acceleration \mathbf{a} of Lagrangian form is

$$\mathbf{a} = \mathbf{a}_N + \mathbf{a}_{PN}^{(1)} + \mathbf{a}_{PN}^{(2)} + \mathbf{a}_{PN}^{(2.5)}, \quad (16)$$

the expressions of \mathbf{a} can be found in citations [35–37].

$$\begin{aligned} \mathbf{a}_{PN}^{(2.5)} = & \frac{8}{5} \left(\frac{\eta}{r} \right) \left\{ \frac{\mathbf{n}}{r} [(\mathbf{r} \cdot \mathbf{p}) \left(\frac{17}{13r} + 3p^2 + \frac{9}{2}(3\eta - 1)p^4 \right. \right. \\ & - \frac{1}{2} \left(5\eta + \frac{179}{3} \right) \frac{p^2}{r} - \frac{1}{3} (25\eta + 51) \frac{1}{r^2} - 6\eta \frac{(\mathbf{n} \cdot \mathbf{p})^2}{r}] \\ & - \frac{\mathbf{p}}{r^2} \left[\frac{3}{r} + p^2 + \frac{3}{2}(3\eta - 1)p^4 + \frac{1}{2}(3\eta - 21) \frac{p^2}{r} \right. \\ & \left. \left. - 3(3 + \eta) \frac{1}{2} - 2\eta \frac{(\mathbf{n} \cdot \mathbf{p})^2}{r} \right] \right\} \end{aligned} \quad (17)$$

Here we choose Hamiltonian to avoid chaotic results by Lagrangian form [38]. The conserved 2.5PN Hamiltonian in the relative coordinate is

$$\mathcal{H}(\mathbf{r}, \mathbf{p}) = \mathcal{H}_N + \mathcal{H}_{PN}^{(1)} + \mathcal{H}_{PN}^{(2)}. \quad (18)$$

To obtain the trajectory of binaries, we need to calculate high order expansions of Hamiltonian equations [39, 40], the derivatives of \mathcal{H} respective to the total momentum p are

$$\frac{\partial \mathcal{H}}{\partial p_N} = p, \quad (19)$$

$$\frac{\partial \mathcal{H}^{(1)}}{\partial p_{PN}} = \frac{1}{2} (3\eta - 1)p^3 - \frac{1}{2} [(3 + \eta)2p + \eta \cos \phi] \frac{1}{r}, \quad (20)$$

$$\begin{aligned} \frac{\partial \mathcal{H}^{(2)}}{\partial p_{PN}} = & \frac{1}{4} (1 - 5\eta + 5\eta^2)p^3 + \frac{1}{4} [-8\eta^2 p^3 \cos^2 \phi \\ & + (5 - 20\eta - 3\eta^2)p^2 - 12\eta^2 p^3 \cos^4 \phi] \frac{1}{r} \\ & + \frac{1}{2} [(5 + 8\eta)2p + 6\eta \cos^2 \phi] \frac{1}{r^2}, \end{aligned} \quad (21)$$

and those respective to r are

$$\frac{\partial \mathcal{H}}{\partial r_N} = \frac{1}{r^2}, \quad (22)$$

$$\frac{\partial \mathcal{H}^{(1)}}{\partial r_{PN}} = \frac{1}{2} [(3 + \eta)p^2 + \eta p \cos \phi] \frac{1}{r^2} - \frac{1}{r^3}, \quad (23)$$

$$\begin{aligned} \frac{\partial \mathcal{H}^{(2)}}{\partial r_{PN}} = & - \frac{p^2}{8r^2} [(5 - 20\eta - 3\eta^2) - 2\eta^2 p^2 \cos^2 \phi \\ & - 3\eta^2 p^2 \cos^4 \phi] + [(5 + 8\eta)p^2 \\ & + 3\eta p^2 \cos^2 \phi] \frac{1}{r^3} - \frac{3}{4} (1 + 3\eta) \frac{1}{r^4}, \end{aligned} \quad (24)$$

where ϕ is the angular separation between \mathbf{r} and \mathbf{p} , imply $\mathbf{r} \cdot \mathbf{p} = rp \cos \phi$. Those dynamical equations are highly nonlinear partial differential equations, which are difficult to solve analytically [41], so we turn to numerical solutions.

C. Gravitational Wave Form

In order to obtain the complete GWF, we consider binaries merge to form a black hole. The evolutionary process of binary systems can be generally divided into three phases as inspiral-merger-ringdown. The GW h^{IM} during inspiral and merger can be calculated by post-Newtonian approximation, and that of ringdown h^{RD} calculated by black hole perturbation theory [42], where t_0 is the time of merger.

$$h = h^{IM} \Theta(t_0 - t) + h^{RD} \Theta(t - t_0), \quad (25)$$

where Θ is jump function of t . In late ringdown trailing phase, we have [43–45]:

$$h^{RD} = \frac{8\mu}{R} \sqrt{\frac{\pi}{5}} e^{-im\phi} H^{RD}, \quad (26)$$

where R is the distance from the source, and for the GW150914 we have $R = 1.768 \times 10^{20} R_\odot$. When it is far enough the above equation can be approximated as

$$h^{RD} = \frac{8\mu}{R} \sqrt{\frac{\pi}{5}} e^{-\frac{\pi f t}{2}} \cos(2\pi f t), \quad (27)$$

$$\mathcal{Q} = 2(1 - a_*)^{-\frac{9}{20}} = 2(1 - \frac{c\mathbf{J}}{GM^2})^{-\frac{9}{20}}. \quad (28)$$

$$a_* = c\mathbf{J}/GM^2 = \mathbf{J}/M^2, \quad (29)$$

a_* is the spin rate of black hole [46]. The angular momentum $\mathbf{J} = \mathbf{r}_i \cdot \mathbf{p}_i$, where \mathbf{r}_i , \mathbf{p}_i is the winding radii and momentum of binaries. The usual compact binary systems in the Milky Way, GS2000+25 and LMC X-3 systems, their spin rate $a_* = 0.03$ [47].

The Newman-Penrose formalism [48] can be obtained from the two independent polarization modes h_\times and h_+ . At infinity from the wave source, all gravitational radiative degrees of freedom are contained a master wave equation of the Weyl scalars ψ_n ($n = 0, 1, 2, 3, 4$) [49, 50], where only ψ_4 remains in significance

$$\psi_4(t) = \frac{\partial^2}{\partial t^2} (h_+(t) - ih_\times(t)), \quad (30)$$

It indicates that the complex Weyl scalar ψ_4 are determined by the second derivative of h_+ and h_\times with respect to time.

We use the mass quadrupole tensor to express h_{ij} with the higher-order expansions of \mathcal{H} [51].

$$\begin{aligned} h_{ij} = & \frac{2\mu r}{R} [\mathcal{H}_{ij}^{(0)} + r^{1/2} \mathcal{H}_{ij}^{(1/2)} + r^1 \mathcal{H}_{ij}^{(1)} \\ & + r^{3/2} \mathcal{H}_{ij}^{(3/2)} + r^2 \mathcal{H}_{ij}^{(2)} + \mathcal{O}(\frac{1}{c^5})]_{TT}. \end{aligned} \quad (31)$$

And the two polarization modes of GW [52] are

$$h_+ = \frac{4M_c^{\frac{5}{3}}}{R} (\pi f_{GW})^{\frac{2}{3}} \frac{1 + \cos^2 \phi}{2(1 - e^2)} \cos(2\pi f_{GW} t + \varphi), \quad (32)$$

$$h_\times = \frac{4M_c^{\frac{5}{3}}}{R} (\pi f_{GW})^{\frac{2}{3}} \frac{\cos \phi}{(1 - e^2)} \sin(2\pi f_{GW} t + \varphi), \quad (33)$$

where ϕ is the deflection angle of binaries and f_{GW} is the radiation frequency of GW [20, 53], which is mainly defined by M_c and $\tau = t - t_0$.

$$f_{GW}(\tau) = \frac{1}{8\pi} \left(\frac{5}{\tau}\right)^{\frac{3}{8}} M_c^{\frac{5}{8}} \quad (34)$$

where M_c is the chirpmass.

$$M_c = (m_1 m_2)^{3/5} (m_1 + m_2)^{-1/5}. \quad (35)$$

The frequency of GW is twice of inspiral frequency $f_{GW} = 2f$. Since mass-transfer mainly happens in inspiral and merger, our discussion on the GWF and binary evolution correction are focus ed on that period. To make the whole process more complete, we extend our GWF to ringdown phase h^{RD} , which also varies as the mass-transfer correction is applied to common envelope evolution mode.

D. Binary System Evolution Equations

Based on the results above, we set the gravitational potential E , winding frequency f , and rotation period T as functions of time. Plugging into formulas we get the radiation power P and the waveform of h_+ and h_\times . Further more, we obtain the trajectory of binary stars according to their radii r_1 and r_2 .

The canonical Hamiltonian equation which is guaranteed to be convergent is

$$\frac{dr}{dt} = \frac{\partial \mathcal{H}}{\partial p}, \quad (36)$$

$$\frac{dp}{dt} = -\frac{\partial \mathcal{H}}{\partial r} + a_{PN}^{(2.5)}. \quad (37)$$

From that we have evolution equations of orbit parameters taking spin $\mathbf{S} = 0$ in Eulerian form[54, 55]

$$\frac{da}{dt} = -\frac{64}{5} \frac{\mu M^2}{a^3 (1-e^2)^{\frac{7}{2}}} \left(1 + \frac{73}{24} e^2 + \frac{37}{96} e^4\right), \quad (38)$$

$$\frac{de}{dt} = -\frac{304}{15} \frac{e \mu M^2}{a^4 (1-e^2)^{\frac{5}{2}}} \left(1 + \frac{121}{304} e^2\right), \quad (39)$$

$$\frac{dE}{dt} = -\frac{8}{15} \frac{m_1^2 m_2^2 M}{a^5 (1-e^2)^5} b^4 (12b^2 + e^2 \sin \theta), \quad (40)$$

$$\frac{dT}{dt} = -\frac{96}{5} \frac{T \mu M^2}{a^4 (1-e^2)^{\frac{7}{2}}} \left(1 + \frac{73}{24} e^2 + \frac{37}{96} e^4\right). \quad (41)$$

Here we set the initial values

$$\begin{aligned} m_1 &= 2M_\odot, \quad m_2 = 1.4M_\odot, \\ a &= r = 25R_\odot, \\ |v_0| &= 1 \times 10^{-4}, \\ \theta &= 0, \\ e &= 0.1, 0.3, 0.6. \end{aligned}$$

4th-order Rounge-Kutta method is used to numerically solve those differential equations. The GWFs are shown as follows by plugging data into formulas. A comparative figure of different initial eccentricities of NS-NS binaries without mass-transfer is given in FIG.1.

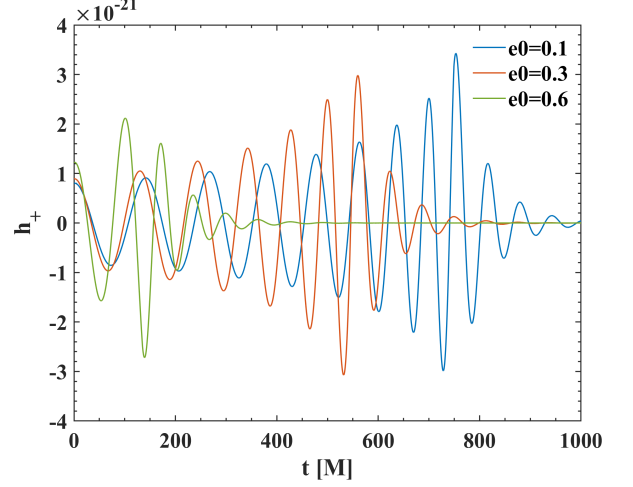


FIG. 1. The figure shows GWs with different initial eccentricities $e = 0.1, 0.3, 0.6$. Fixing the initial distance, when the eccentricity gets larger, binaries tend to merge more quickly, while the GWs in ringdown phase are basically unaffected.

IV. MASS TRANSFER CORRECTION

A. Mass Quadrupole Correction

We establish a model where there is a stable and conservative mass-loss flow between two stars, whose quadrupole tensor can be written as

$$Q'_{ij} = \frac{m_0}{3} \left[1 - \frac{3m_1 m_2}{M^2}\right] L^2 W \omega, \quad (42)$$

$$W_{ab} = \begin{pmatrix} \cos 2\theta & \sin 2\theta \\ \sin 2\theta & -\cos 2\theta \end{pmatrix}, \quad \varphi \equiv 2\theta, \quad (43)$$

$$\ddot{W}_{ab} = \begin{pmatrix} -\ddot{\varphi} \sin \varphi - \dot{\varphi}^2 \cos \varphi & \ddot{\varphi} \cos \varphi - \dot{\varphi}^2 \sin \varphi \\ \ddot{\varphi} \cos \varphi - \dot{\varphi}^2 \sin \varphi & \ddot{\varphi} \sin \varphi + \dot{\varphi}^2 \cos \varphi \end{pmatrix}, \quad (44)$$

$$\ddot{Q}'_{ij} \approx \frac{m_0}{3} L^2 \ddot{W}, \quad \ddot{Q}_{ij} = \ddot{Q}_{ij}^0 + \ddot{Q}'_{ij}, \quad (45)$$

where Q_{ij}^0 is the mass quadrupole of the two stars without mass-transfer, and L is length of the mass-transfer flow.

On this basis we theoretically conceive the following two models of mass-transfer: the tidal disruption model and the common envelope evolution model, which are illustrated in Fig.2.

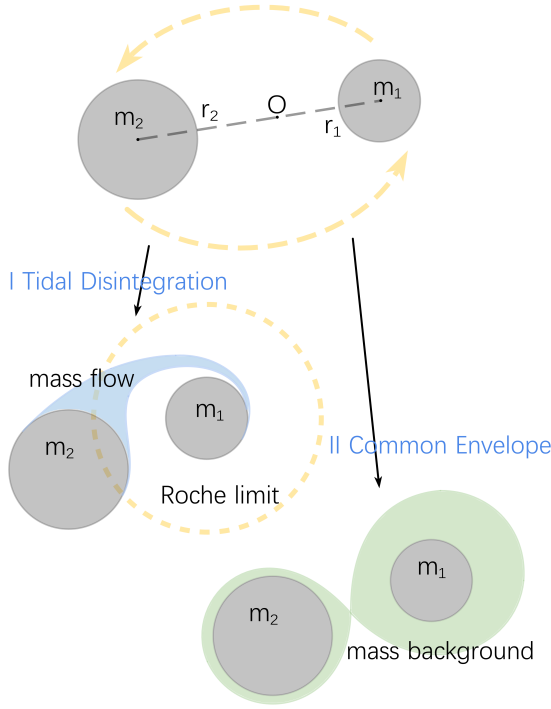


FIG. 2. At the top of figure is the compact binaries in inspiral, where the mass of m_1 is more compact than m_2 . Below are two mass-transfer models, the left one is the case with tidal disruption only, and the right one is the case of common envelope evolution, which divides the mass-loss flow into mass-inflow and mass-background in the Roche lobe of m_1 . The real astro process is usually the combination of those two.

B. Tidal Disruption

Considering a direct in-compressible flow of mass-loss from m_2 to m_1 in the Roche limit of the more massive star, where the mass flow sums to m_1 after a rapid orbit. In order to represent the strength of the mass-transfer, we introduced the Euler equations for in-compressible fluids [56, 57].

$$\frac{dm_2}{dt} = \frac{dm_2}{dv} \cdot \frac{dv}{dt} = \frac{dV}{dv} \cdot \rho \frac{dv}{dt} = \frac{1}{\delta v} F_T, \quad (46)$$

$$\rho \frac{dv}{dt} = -\nabla P_p + \rho \tilde{g}, \quad (47)$$

where P_p is the pressure of mass flow and in this situation $P_p=0$, \tilde{g} is the gravitational acceleration defined by the tidal gravity. δv is the change of velocity of mass transfer flow in a short time δt , so that we have $\delta v = a\delta t$. Define d as the distance of binaries, and then get

$$\frac{1}{\delta v} = \frac{(d_1 d_2)^2}{(m_1 d_2^2 - m_2 d_1^2) \delta t}, \quad (48)$$

where d_1, d_2 are the distance from a infinitesimal of the mass-transfer flow to m_1, m_2 . The mass changes of two stars are due to tidal disruption [58]. According to above calculation we know that $F_T = \rho \tilde{g} dV$, which strongly

related to the tidal gravity, so that F_T can be described as an analytical function

$$F_T = \frac{M\mu}{(d-R_0)^2} - \frac{M\mu}{d^2} = \frac{M\mu(2dR_0 - R_0^2)}{d^4 - 2d^3R_0 + R_0^2d^2}, \quad (49)$$

R_0 is the radius of m_2 . Use tidal gravity as a mass transfer function, we can obtain the mass change in the system at this time.

$$m'_1 = m_1 + \alpha \frac{m_1 m_2 R_0}{2(m_1 - m_2)(d - R_0)\delta t} \quad (50)$$

$$m'_2 = m_2 - \frac{m_1 m_2 R_0}{2(m_1 - m_2)(d - R_0)\delta t} \quad (51)$$

where $0 \leq \alpha \leq 1$ is the mass-inflow parameter, implying $\dot{m}_1 = \alpha \dot{m}_2$. In this section we set $\alpha = 1$, which means the total mass of the binaries is conserved.

Consider a static, spherically symmetric star of mass m placed in a external quadrupole tidal field ϵ_{ij} , which is a function of F_T . The star will develop in response a quadrupole tensor Q_{ij} [58, 59].

$$g_{ij} = 1 - 2\left[-\frac{m}{r} - \frac{3Q_{ij}}{2r^3}\left(\frac{x^i x^j}{r^2} - \frac{\delta_{ij}}{3}\right) + \frac{F_T}{2r} x^i x^j\right]. \quad (52)$$

The expression for the change of the Weyl scalar is

$$\delta\psi_4 = -\frac{9(\pi M f)^{\frac{5}{3}}}{16\mu M^4} \left[\left(11\frac{m_1}{m_2} + \frac{M}{m_1}\right) \frac{1}{r\delta v} + 1 \leftrightarrow 2 \right]. \quad (53)$$

At the same time, define $q' = m_2/m_1 = 1/q$ the conservative evolution of inspiral semi-major axis and GW frequency with mass transfer can be obtained [60]

$$\frac{da}{dt} = -\frac{64\mu M^2 a^{-3}}{5(1-e^2)^{\frac{7}{2}}} \left(1 + \frac{73}{24}e^2 + \frac{37}{96}e^4\right) - 2aC\frac{\dot{m}_2}{m_2}, \quad (54)$$

$$\frac{df}{dt} = \frac{96}{5}\pi^{\frac{8}{3}}m_1 m_2 M^{-\frac{1}{3}} + 3fC^{-1}\frac{\dot{m}_2}{m_2}, \quad (55)$$

$$C = [1 - \alpha q' - (1 - \alpha) \frac{q'}{q' + 1} - \alpha \sqrt{1 + q'}]^{-1}. \quad (56)$$

Here, the influence of tidal effects is a small correction to the GW inspiral phase in $(2.0 + 1.4)M_\odot$ NS-NS binaries, and the radii of NSs is about $R_0 \cong 3 \times 10^{-5}R_\odot$, which means there is no tidal disruption until the NS-NS binaries close enough. So that we establish a $(2.0 + 0.5)M_\odot$ NS-WD system, and the radius of WD is $R_0 \cong 1 \times 10^{-2}R_\odot$. The formula of mass-transfer correction is brought into the coupled differential equation system solved in the last section. And the results are shown in Fig.3.

In order to facilitate the investigation of the underlying causes of the variation of GW, we simultaneously plot the evolution of dynamical parameters of the $(2.0 + 0.5)M_\odot$ NS-WD system, including the radiation power, the orbital eccentricity, and the orbital radius. The radiation power increases significantly as it approaches the merger,

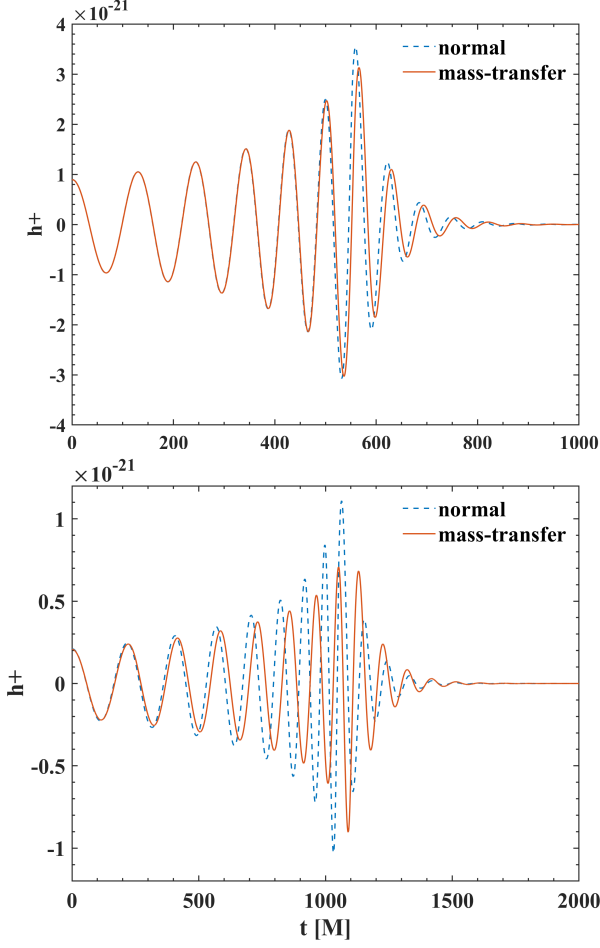


FIG. 3. The upper figure is the GW in the inspiral phase of NS-NS binaries with a small change, due to the small q , R_0 , and Roche limit. The lower figure is NS-WD binaries, which shows that the highest peak of its GW strength decreases, while the merger time is delayed. The degree of change in NS-WD is significantly greater than that in NS-NS and the mass-transfer process occurred earlier.

so its natural logarithmic value is used as the vertical coordinate of FIG. 4. The main difference is reflected in the late inspiral phase, when m_2 in the Roche limit of m_1 .

The figure shows that the radiation power of the system decreases with the mass-transfer correction, while the effect on the orbital eccentricity is smaller. The lower left corner shows the orbital radius of the more compact star, which decreases the orbital radius more quickly relative to the previous one after receiving the transferred mass, while the opposite changes for the other star.

C. Common Envelope

We consider that in addition to the direct mass-transfer flow between two stars [31, 53], a part of the mass-loss forms a common envelope between the binary

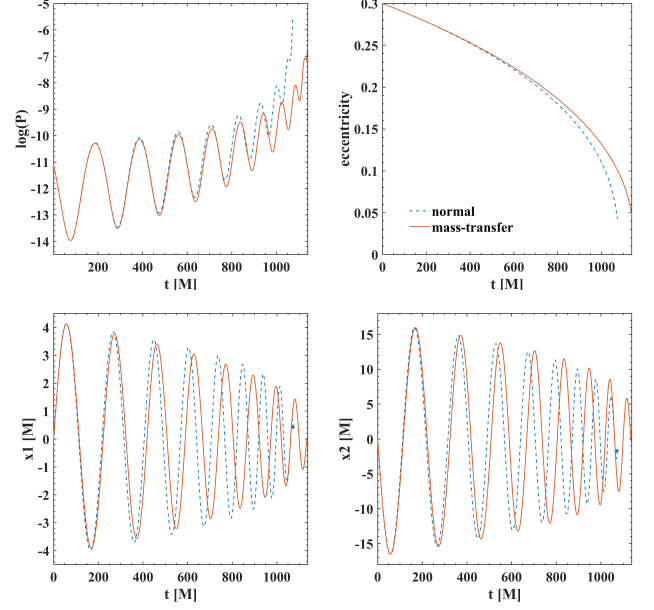


FIG. 4. Time evolution of individual dynamical parameters of NS-WD binaries system with the mass-transfer correction. The blue point in the two figures of x_1 and x_2 (abscissa of NS and WD) are merger points without mass-transfer.

stars similar as mass-background in Roche lobe of NS. This part of mass is in the system but does not belong to the NS, and because of its regular and symmetric mass distribution, we consider it as a third non-spherically symmetric single-star system in spin motion.

The mass-background will be concentrated in a certain area, and the Roche lobe radius [61] of this area is

$$r_L(q) = \frac{0.49q^{2/3}}{0.6q^{2/3} + \ln(1 + q^{1/3})}. \quad (57)$$

For the case of an ellipsoidal neutron star with uniform mass spin [62], the variation of the spin period is influenced by the accretion process while radiating GWs with radiation power of

$$P = \dot{E}_{GW} = -\frac{32}{5}I^2e^2\omega^6, \quad (58)$$

$$\omega = \left(\frac{5\dot{M}}{64I^2e^2}\sqrt{RR_A}\right)^{1/2}, \quad (59)$$

where ω is angular velocity of neutron star spin, I is the rotational inertia, and R_A is the Alvin Radius. So that we can get the equation of h in inspiral phase combine with compact binaries orbiting and spin of mass-background. $H(t)$ is the expression of the spin GW strength, which can be expanded to 3PN order [63].

$$h_+ = h_+^{In} + H(t)e^{-im\phi_{orb}t}. \quad (60)$$

In the case of the common envelope evolution, we need to consider the part of the mass-inflow from m_2 to m_1 ,

and the others becomes the mass-background. Determine the stability of mass-transfer in NS-WD systems based on the exponent of the adiabatic mass-radius of the planet

$$\zeta_P = \partial \ln r_p / \partial \ln \dot{M}, \quad (61)$$

and its corresponding exponent of the NS Roche lobe radius r_L with respect to the NS mass [64, 65]

$$\zeta_L = \partial \ln r_L / \partial \ln \dot{M}. \quad (62)$$

And if $\zeta_P - \zeta_L > 0$, we think it is a stable mass-transfer process.

So that $\alpha = \delta m_1 / \delta m$ are defined here, where δm is the mass-loss of WD and δm_1 is the mass-inflow to NS. The mass inflow parameter α can be defined as [60, 66]

$$\alpha \equiv \partial \ln \dot{m}_1 / \partial \ln r, \quad (63)$$

$$\alpha(\eta_w, \gamma) = \frac{1}{2} [1 - \eta\gamma + (-5\gamma^2 + 10\eta\gamma^2 + \eta^2\gamma^2 + 6\gamma)^{1/2}] / (-\gamma + 2\eta\gamma + 1), \quad (64)$$

where $\gamma = 5/3, 4/3$ is an adiabatic index, and η_w is the winding efficiency parameter. We know that for a $(1.4 + 0.1)M_\odot$ NS-WD system, $\alpha \gtrsim 0.5$ of the mass-loss of WD can be accreted by its companion NS, while for $(1.4 + 1.25)M_\odot$ NS-WD system, the accretion parameter α drops steeply to 5.4×10^{-4} [60]. According to this data compare to FIG.5, we can relate q to η_w linear, and get the function $\alpha(q, \gamma)$ to replace η_w . In the following calculation we set $\gamma = 5/3$.

The results are shown in Fig.5. When the NS-WD binaries has $q = 4$, we get $\alpha = 0.1662$ to this system. The difference of the GWs due to the common envelope evolution is more obvious compared to the case of tidal disruption. It is mainly reflected in the decrease of the GW strength and delay of the merger time.

In Fig.6 we calculate the orbital trajectory of the NS-WD binaries. Since the initial mass ratio $q = 4$, winding radius of WD is about 4 times as long as NS. As time goes on, the change rate of winding radius increases until merger. When the mass-transfer correction is added, the binaries' orbit changes differently, the NS received the mass-transfer decreasing the orbital radius more quickly and converging to the center of the orbit, while WD which lost mass will be farther away from the center with a relatively large orbital radius.

So that the mass-transfer is an important factor, which has obvious significance to the orbits and GWs of NS-WD binaries, especially at the late inspiral phase, which is close to merger.

D. Binary Systems with Different Mass Ratios

In above words, we mainly discussed compact NS-WD binary systems with initial mass ratio $q = m_1/m_2 = 4$. In the real case, there are still binaries with larger or smaller mass ratios [67, 68], and we combine the mass

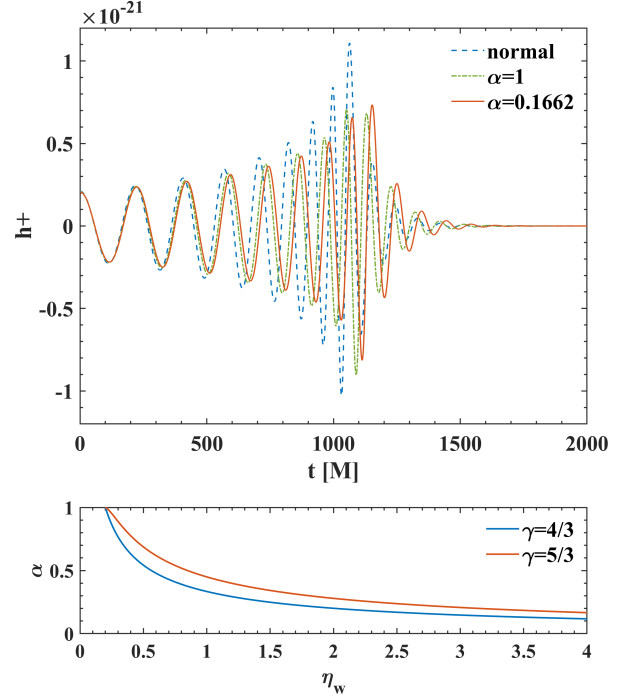


FIG. 5. The upper figure shows the GWs of NS-WD binaries with mass-inflow parameter α , we can see the decrease of GW strength and frequency reduction, which cause the delay of merger time. And the GWs of ringdown phase are depend on the merger momentum and frequency. The lower figure shows the mass-inflow parameter α function of η_w , to this system correspond to $\eta_w = 4$ and then get $\alpha = 0.1662$.

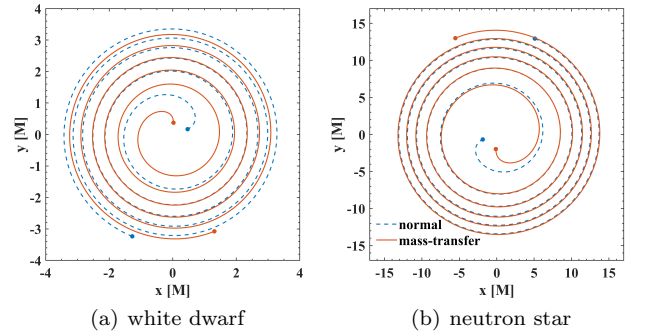


FIG. 6. In order to discuss the orbital differences caused by mass transfer more clearly, we intercept the evolution time $t = 500 \sim 1000[M]$ close and plot the data in the inspiral phase, WD's orbit on the left and NS's orbit on the right. Because of the difference in mass, the winding radius of WD is about 4 times as long as NS.

transfer correction to calculate the GWs in three cases: $(2 + 0.5)M_\odot$, $(2 + 0.7)M_\odot$, and $(2 + 1.0)M_\odot$ NS-WD binaries in FIG.7. In addition to affecting the Roche limit of NS, different q will also correspond to different α .

In order to get the information of $m_1(t)$ and $m_2(t)$, we get the mass change curve in FIG.8. We can intuitively

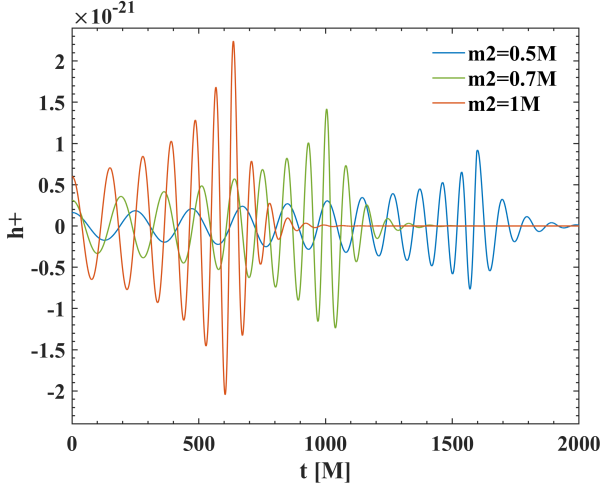


FIG. 7. In the case of initial mass ratio $q = 4, 20/7, 2$, starting from the distance $d = 23R_\odot$, the difference is in the merger time and the strength of GW. It is obvious that, with the increase of q , the merger time is significantly earlier, while the strength of GW increases greatly.

see that the mass transfer occurs earlier for WD systems with smaller masses corresponding to the larger Roche limit, and the masses received by NS (final mass) are all similar. However, there is a significant difference in the lost mass for WDs, with smaller masses losing a larger percentage of their mass instead. Combined with the variation of the mass-inflow parameter α , this conclusion is reasonable because WD with smaller masses will have smaller α . In the process of mass transfer, it can be found that the step shape at the beginning of the mass change is due to the eccentricity causing the binary distance to oscillate above and below the Roche limit, and the mass transfer only occurs when it is within the Roche limit. As the distance between NS-WD binaries decreases, the mass transfer rate becomes larger.

TABLE I. mass-transfer of NS-WD binaries

NS-WD	m_1 [M]	m_2 [M]	$\delta m/m_2$	α
$(2 + 0.5)M_\odot$	2.0194	0.3834	0.395	0.166
$(2 + 0.1)M_\odot$	2.0189	0.6119	0.199	0.215
$(2 + 1.0)M_\odot$	2.0191	0.9318	0.095	0.279

We record the final mass of NS-WD, $\delta m/m$, and mass-inflow parameter α in TAB.I. The mass-loss rate is $0.395 \sim 0.095$ with the mass of WD $0.5 \sim 1.0M_\odot$, which means the smaller mass WD is the stronger mass-loss will be. Metzger [69] used one-dimensional steady-state models of accretion discs produced by the tidal disruption of a WD by an NS or a black hole, and find that at the high accretion rates of $10^{-4} \sim 10^{-1}M_\odot/s$, this matches our conclusion well.

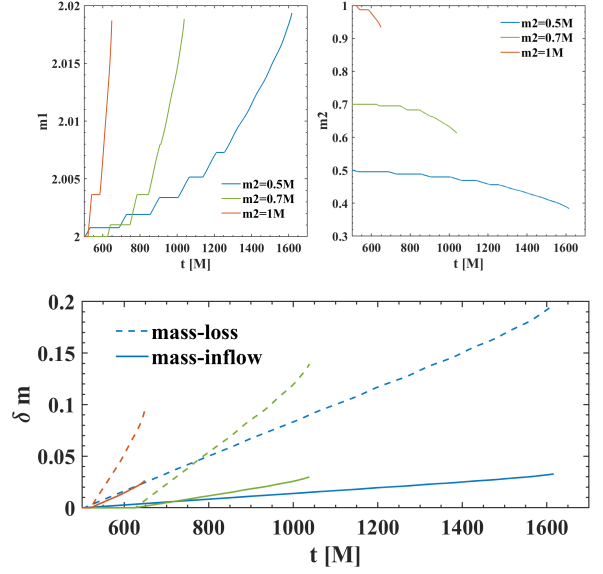


FIG. 8. In different NS-WD systems, the larger the WD mass is, the later the binaries will occur mass-transfer process, means the smaller Roche limit. As seen in the lower figure, the lower the mass of the WD, the less mass-transfer becomes mass-inflow, while the greater part becomes mass-background within the Roche lobe of the NS.

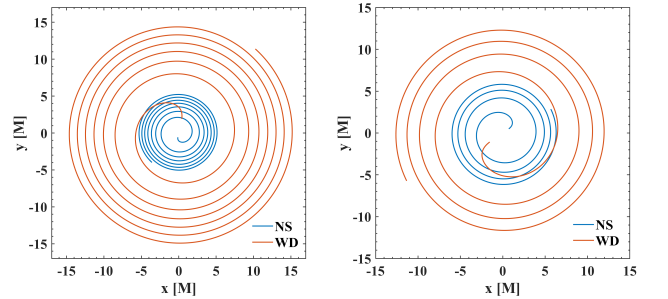


FIG. 9. The calculation of the orbit of $(2 + 0.7)M_\odot$ (left) and $(2 + 1.0)M_\odot$ (right) NS-WD binaries. The initial distance of the binary star is $d = 23R_\odot$, and the orbits of $t > 500[M]$ is shown in the figure. When the masses of the binary stars are more similar, the orbit radius is also higher symmetry.

We calculated the orbit of $(2 + 0.7)M_\odot$ and $(2 + 1.0)M_\odot$ NS-WD binaries in FIG.9, the winding radii ratio of NS and WD is proportional to q . When q is large, the trajectory of the binaries is more inclined to WD wind around, while NS is relatively stable in the middle. In a more extreme case, it would be similar to the relationship of the central object to the orbiting planet, which takes longer time to merger. In the case of NS-NS systems, the binary stars have similar masses and radii, and their trajectories will exhibit a centrosymmetric pattern.

To sum up, as the mass ratio increases the binaries tend to merge more quickly and the number of revolu-

tions decreases significantly. At the same time, the increased mass of one of the stars leads to an increase in the rate of change of the mass quadrupole tensor, and the gravitational radiation power and GW intensity during the whole inspiral phase also increase. For the ringdown phase, the change from an asymmetric to a symmetric sphere is also faster when q increases, so that the duration of ringdown is significantly reduced.

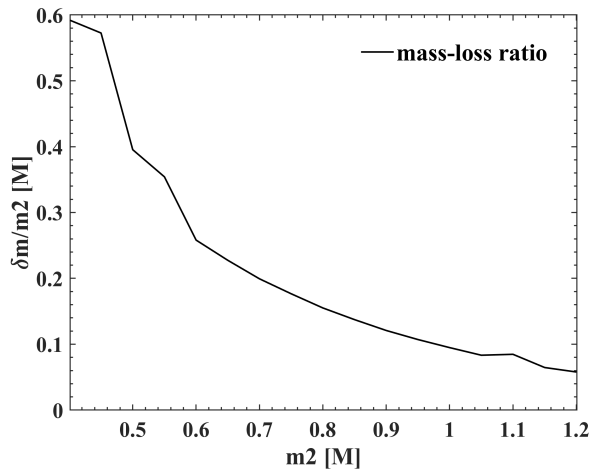


FIG. 10. Mass of WD changes from $0.4M_\odot$ to $1.2M_\odot$, which is almost the mass range of a white dwarf in theory and detection. When $m_2 \gtrsim 0.45M_\odot$, $\delta m/m_2$ varies exponentially with m_2 , and the change ratio of $\delta m/m_2$ becomes smaller and stable at about 0.6 when the mass reduce smaller than $0.4M_\odot$.

Further more, in order to check the convergence of the whole model, we let the mass of WD goes from $0.4M_\odot$ to $1.2M_\odot$ in FIG.10, when the general white-dwarf mass between $0.493M_\odot$ and $1.05M_\odot$ [70]. We can see that, the mass-loss ratio is decrease in exponential form. When $m_2 \rightarrow m_1 = 2M_\odot$, this system just become NS-NS system basically no mass-transfer. When the WD mass reduce to $0.45M_\odot$, the mass-transfer ratio reaches 0.5725, and the change ratio of $\delta m/m_2$ becomes smaller and stable at about 0.6 when the mass reduce smaller than

$0.4M_\odot$, which also ensures the convergence when the WD mass is small.

V. CONCLUSIONS

For the tidal disruption type of mass-transfer, the overall variation of NS-NS binaries' GWs are small, while a larger change occurs when the mass-loss is divided into mass-background and mass-inflow of NS-WD binaries. We have theoretically derived the equation for mass-transfer by tidal gravity, and then added the mass-inflow parameter α to calculate the various types of mass evolution in the binary system and its corresponding GWs. We set the massive NS $m_1 = 2M_\odot$, and WD $m_2 = 0.4 \sim 1.2M_\odot$, got the $\alpha = 0.1393 \sim 0.3204$ and mass-loss $\delta m/m_2 = 0.5923 \sim 0.0578$. These results are consistent with the detection data now, and the calculation is convergent in all the mass ranges of WD.

The dynamical evolution of a NS-WD system has more physical processes than a binary black hole system. We have effectively and reasonably simplify the independent variables and the mass distribution, and give the GWs in various cases by different theoretical bases, which constitute a more comprehensive library of GWs templates.

When using the post-Newton approximation to calculate the mass-transfer correction, cause the NS-NS binaries does not have a significant effect on the waveform, so that we focus on the NS-WD binaries, which has larger q and Roche limit. This result is caused by the limitation of the post-Newton approximation in the merger period. In the subsequent studies, we prefer to use Numerical-Relativity to deal with the merger period, which can improve the computational accuracy while a more widely applicable mass transfer model can be obtained.

VI. ACKNOWLEDGMENTS

We thank professor Jie Yang for his guidance and support in the theoretical basis of the academic research about the mass-transfer of binaries.

-
- [1] T. Regimbau and S. A. Hughes, Gravitational-wave confusion background from cosmological compact binaries: Implications for future terrestrial detectors, *Phys. Rev. D* **79**, 062002 (2009).
 - [2] B. Liu and D. Lai, Probing the spins of supermassive black holes with gravitational waves from surrounding compact binaries, *The Astrophysical Journal* **924**, 127 (2022).
 - [3] V. Baibhav, E. Berti, D. Gerosa, M. Mapelli, N. Giacobbo, Y. Bouffanais, and U. N. Di Carlo, Gravitational-wave detection rates for compact binaries formed in isolation: Ligo/virgo o3 and beyond, *Phys. Rev. D* **100**, 064060 (2019).
 - [4] V. D. Luca, G. Franciolini, P. Pani, and A. Riotto, The minimum testable abundance of primordial black holes at future gravitational-wave detectors, *Journal of Cosmology and Astroparticle Physics* **2021**, 039 (2021).
 - [5] E. Berti, L. Gualtieri, M. Horbatsch, and J. Alsing, Light scalar field constraints from gravitational-wave observations of compact binaries, *Phys. Rev. D* **85**, 122005 (2012).
 - [6] S. Babak, R. Balasubramanian, D. Churches, T. Cokelaer, and B. S. Sathyaprakash, A template bank to search for gravitational waves from inspiralling compact bina-

- ries: I. physical models, [Classical and Quantum Gravity](#) **23**, 5477 (2006).
- [7] T. Cokelaer, A template bank to search for gravitational waves from inspiralling compact binaries: Ii. phenomenological model, [Classical and Quantum Gravity](#) **24**, 6227 (2007).
- [8] M. Shibata, K. Kyutoku, T. Yamamoto, and K. Taniguchi, Erratum and addendum: Gravitational waves from black hole-neutron star binaries: Classification of waveforms, [Phys. Rev. D](#) **85**, 127502 (2012).
- [9] M. Shibata, K. Kyutoku, T. Yamamoto, and K. Taniguchi, Gravitational waves from black hole-neutron star binaries: Classification of waveforms, [Phys. Rev. D](#) **79**, 044030 (2009).
- [10] T. Wagg, F. S. Broekgaarden, S. E. de Mink, N. Frankel, L. A. C. van Son, and S. Justham, Gravitational wave sources in our galactic backyard: Predictions for bhh, bhns, and nsns binaries detectable with lisa, [The Astrophysical Journal](#) **937**, 118 (2022).
- [11] B. McKernan, K. E. S. Ford, and R. O’Shaughnessy, Black hole, neutron star, and white dwarf merger rates in AGN discs, [Monthly Notices of the Royal Astronomical Society](#) **498**, 4088 (2020).
- [12] C. Hamilton and R. R. Rafikov, Anatomy of a slow merger: Dissecting secularly driven inspirals of ligo/virgo gravitational wave sources, [The Astrophysical Journal](#) **939**, 48 (2022).
- [13] G. M. Kremer, Stellar structure model in the post-newtonian approximation, [Research in Astronomy and Astrophysics](#) **22**, 125009 (2022).
- [14] L. Blanchet, S. Detweiler, A. Le Tiec, and B. F. Whiting, Post-newtonian and numerical calculations of the gravitational self-force for circular orbits in the schwarzschild geometry, [Phys. Rev. D](#) **81**, 064004 (2010).
- [15] I. Futamase, Toshifumi, The post-newtonian approximation for relativistic compact binaries, [Living Reviews in Relativity](#) **10.12942/lrr-2007-2** (2007).
- [16] T. Rainsford, Newtonian and post-newtonian approximations of the $k=0$ friedmann–robertson–walker cosmology, [General Relativity and Gravitation](#) **10.1023/A:1001971203318** (2000).
- [17] D. Bini and T. Damour, Analytical determination of the two-body gravitational interaction potential at the fourth post-newtonian approximation, [Phys. Rev. D](#) **87**, 121501 (2013).
- [18] G. Cho, A. Gopakumar, M. Haney, and H. M. Lee, Gravitational waves from compact binaries in post-newtonian accurate hyperbolic orbits, [Phys. Rev. D](#) **98**, 024039 (2018).
- [19] H. W. B. T. Cai R G, Cao Z J, e gravitational wave models for binary compact objects (in chinese)., [hin Sci Bull](#) (2016).
- [20] S. Tanay, M. Haney, and A. Gopakumar, Frequency and time-domain inspiral templates for comparable mass compact binaries in eccentric orbits, [Phys. Rev. D](#) **93**, 064031 (2016).
- [21] J. H. Krolik and I. Linial, Quasiperiodic erupters: A stellar mass-transfer model for the radiation, [The Astrophysical Journal](#) **941**, 24 (2022).
- [22] T. R. Li Yaguang, Bedding, Discovery of post-mass-transfer helium-burning red giants using asteroseismology, [Nature Astronomy](#) **10.1038/s41550-022-01648-5** (2022).
- [23] H.-L. Chen, T. M. Tauris, X. Chen, and Z. Han, Formation of the double white dwarf binary ptf j0533+0209 through stable mass transfer?, [The Astrophysical Journal](#) **925**, 89 (2022).
- [24] Y.-J. Huang, *Numerical simulation for binary neutron star merger and the associated gravitational wave radiation*, [Ph.D. thesis](#), University of Science and Technology of China (2022).
- [25] Y.-J. Huang, L. Baiotti, T. Kojo, K. Takami, H. Sotani, H. Togashi, T. Hatsuda, S. Nagataki, and Y.-Z. Fan, Merger and postmerger of binary neutron stars with a quark-hadron crossover equation of state, [Phys. Rev. Lett.](#) **129**, 181101 (2022).
- [26] P. S. PALMER, Size of fragments resulting from tidal disintegration, [Nature](#) **10.1038/173499a0** (1954).
- [27] R.-X. Yang, F. Xie, and D.-J. Liu, Tidal deformability of neutron stars in unimodular gravity, [Universe](#) **8**, 10.3390/universe8110576 (2022).
- [28] S. Mougiakakos, M. M. Riva, and F. Vernizzi, Gravitational bremsstrahlung with tidal effects in the post-minkowskian expansion, [Phys. Rev. Lett.](#) **129**, 121101 (2022).
- [29] R. G. Izzard, P. D. Hall, T. M. Tauris, and C. A. Tout, Common envelope evolution, [Proceedings of the International Astronomical Union](#) **7**, 95–102 (2011).
- [30] M. E. Beer, L. M. Dray, A. R. King, and G. A. Wynn, An alternative to common envelope evolution, [Monthly Notices of the Royal Astronomical Society](#) **375**, 1000 (2007).
- [31] T. L. S. Wong and L. Bildsten, Mass transfer and stellar evolution of the white dwarfs in am cvn binaries, [The Astrophysical Journal](#) **923**, 125 (2021).
- [32] N. Soker, Spin-orbit misalignment from triple-star common envelope evolution, [Monthly Notices of the Royal Astronomical Society](#) **509**, 2836 (2021).
- [33] D. G. Figueroa, J. Garcia-Bellido, and A. Rajantie, On the transverse-traceless projection in lattice simulations of gravitational wave production, [Journal of Cosmology and Astroparticle Physics](#) **2011**, 015 (2011).
- [34] T. Mora and C. M. Will, Post-newtonian diagnostic of quasiequilibrium binary configurations of compact objects, [Phys. Rev. D](#) **69**, 104021 (2004).
- [35] L. E. Kidder, Coalescing binary systems of compact objects to (post)^{5/2}-newtonian order. v. spin effects, [Phys. Rev. D](#) **52**, 821 (1995).
- [36] H. Tagoshi, A. Ohashi, and B. J. Owen, Gravitational field and equations of motion of spinning compact binaries to 2.5 post-newtonian order, [Phys. Rev. D](#) **63**, 044006 (2001).
- [37] L. Blanchet, A. Buonanno, and G. Faye, Erratum: Higher-order spin effects in the dynamics of compact binaries. ii. radiation field [phys. rev. d 74, 104034 (2006)], [Phys. Rev. D](#) **75**, 049903 (2007).
- [38] X. Wu, L. Mei, G. Huang, and S. Liu, Analytical and numerical studies on differences between lagrangian and hamiltonian approaches at the same post-newtonian order, [Phys. Rev. D](#) **91**, 024042 (2015).
- [39] D. Bini and T. Damour, Gravitational scattering of two black holes at the fourth post-newtonian approximation, [Phys. Rev. D](#) **96**, 064021 (2017).
- [40] M. Ebersold, Y. Boetzel, G. Faye, C. K. Mishra, B. R. Iyer, and P. Jetzer, Gravitational-wave amplitudes for compact binaries in eccentric orbits at the third post-newtonian order: Memory contributions, [Phys. Rev. D](#)

- [100, 084043 \(2019\)](#).
- [41] K. Cannon, C. Hanna, and D. Keppel, Method to estimate the significance of coincident gravitational-wave observations from compact binary coalescence, [Phys. Rev. D **88**, 024025 \(2013\)](#).
 - [42] B. san Sun, *Study of the evolution of double black hole systems with waveform templates*, Ph.D. thesis, Huazhong University of Science and Technology (2015).
 - [43] R. Cotesta, G. Carullo, E. Berti, and V. Cardoso, Analysis of ringdown overtones in gw150914, [Phys. Rev. Lett. **129**, 111102 \(2022\)](#).
 - [44] Y. Boetzel, C. K. Mishra, G. Faye, A. Gopakumar, and B. R. Iyer, Gravitational-wave amplitudes for compact binaries in eccentric orbits at the third post-newtonian order: Tail contributions and postadiabatic corrections, [Phys. Rev. D **100**, 044018 \(2019\)](#).
 - [45] S. A. Hughes, A. Apte, G. Khanna, and H. Lim, Learning about black hole binaries from their ringdown spectra, [Phys. Rev. Lett. **123**, 161101 \(2019\)](#).
 - [46] F. Echeverria, Gravitational-wave measurements of the mass and angular momentum of a black hole, [Phys. Rev. D **40**, 3194 \(1989\)](#).
 - [47] A. R. King and U. Kolb, The evolution of black hole mass and angular momentum, [Monthly Notices of the Royal Astronomical Society **305**, 654 \(1999\)](#).
 - [48] M. Okounkova, L. C. Stein, J. Moxon, M. A. Scheel, and S. A. Teukolsky, Numerical relativity simulation of gw150914 beyond general relativity, [Phys. Rev. D \(2020\)](#).
 - [49] E. T. Newman and R. Penrose, An approach to gravitational radiation by a method of spin coefficients (1962).
 - [50] S. Babak, H. Fang, J. R. Gair, K. Glampedakis, and S. A. Hughes, "kludge" gravitational waveforms for a test-body orbiting a kerr black hole, [Phys. Rev. D **75**, 024005 \(2007\)](#).
 - [51] L. Blanchet, Gravitational radiation from post-newtonian sources and inspiralling compact binaries, [Living Reviews in Relativity **10**.12942/lrr-2002-3 \(2002\)](#).
 - [52] M. Maggiore, *Gravitational Waves Vol 1* (Oxford, 2008).
 - [53] P. Hölscher and D. J. Schwarz, Gravitational waves from inspiralling compact binaries in conformal gravity, [Phys. Rev. D **99**, 084005 \(2019\)](#).
 - [54] P. C. Peters and J. Mathews, Gravitational radiation from point masses in a keplerian orbit, [Phys. Rev. **131**, 435 \(1963\)](#).
 - [55] P. C. Peters, Gravitational radiation and the motion of two point masses, [Phys. Rev. **136**, B1224 \(1964\)](#).
 - [56] A. Gaull, A rigorous proof for the equivalence of the projective newton–euler equations and the lagrange equations of second kind for spatial rigid multibody systems, [Multibody System Dynamics **10**.1007/s11044-018-09639-z \(2019\)](#).
 - [57] N. Nadirashvili, On stationary solutions of two-dimensional euler equation, [Archive for Rational Mechanics and Analysis **10**.1007/s00205-013-0642-8 \(2013\)](#).
 - [58] E. E. Flanagan and T. Hinderer, Constraining neutron-star tidal love numbers with gravitational-wave detectors, [Phys. Rev. D **77**, 021502 \(2008\)](#).
 - [59] K. S. Thorne, Tidal stabilization of rigidly rotating, fully relativistic neutron stars, [Phys. Rev. D **58**, 124031 \(1998\)](#).
 - [60] S. Yu, Y. Lu, and C. S. Jeffery, Orbital evolution of neutron-star–white-dwarf binaries by Roche lobe overflow and gravitational wave radiation, [Monthly Notices of the Royal Astronomical Society **503**, 2776 \(2021\)](#).
 - [61] P. P. Eggleton, Approximations to the radii of roche lobes, [Astrophysical Journal **10**.1086/160960 \(1983\)](#).
 - [62] S. L. Shapiro and S. A. Teukolsky, *Black Holes, White Dwarfs and Neutron Stars* (Wiley-Interscience, 1983).
 - [63] K. G. Arun, A. Buonanno, G. Faye, and E. Ochsner, Erratum: Higher-order spin effects in the amplitude and phase of gravitational waveforms emitted by inspiraling compact binaries: Ready-to-use gravitational waveforms [phys. rev. d **79**, 104023 (2009)], [Phys. Rev. D **84**, 049901 \(2011\)](#).
 - [64] F. D’Antona, I. Mazzitelli, and H. Ritter, The turn-on of mass transfer in cataclysmic binaries, [Astronomy and Astrophysics **225**, 391 \(1989\)](#).
 - [65] P. P. Eggleton, Approximations to the radii of roche lobes, [The Astrophysical Journal **268**, 368 \(1983\)](#).
 - [66] B. Margalit and B. D. Metzger, Time-dependent models of accretion discs with nuclear burning following the tidal disruption of a white dwarf by a neutron star, [Monthly Notices of the Royal Astronomical Society **461**, 1154 \(2016\)](#).
 - [67] A. H. Nitz and Y.-F. Wang, Search for gravitational waves from high-mass-ratio compact-binary mergers of stellar mass and subsolar mass black holes, [Phys. Rev. Lett. **126**, 021103 \(2021\)](#).
 - [68] P. R. Brady and S. A. Hughes, Central density of a neutron star is unaffected by a binary companion at linear order in μ/R , [Phys. Rev. Lett. **79**, 1186 \(1997\)](#).
 - [69] B. D. Metzger, Nuclear-dominated accretion and subluminal supernovae from the merger of a white dwarf with a neutron star or black hole, [Monthly Notices of the Royal Astronomical Society **419**, 827 \(2011\)](#).
 - [70] A. D. Romero, S. O. Kepler, S. R. G. Joyce, G. R. Lauffer, and A. H. Corsico, The white dwarf mass–radius relation and its dependence on the hydrogen envelope, [Monthly Notices of the Royal Astronomical Society **484**, 2711 \(2019\)](#).